Feasibility of Snowpack Characterization Using Remote Sensing and Advanced Data Assimilation Techniques

Principal Investigator
Steven A. Margulis, Assistant Professor
Department of Civil and Environmental Engineering, UCLA
5732D Boelter Hall
UCLA
Los Angeles, CA 90095
Phone: 310-267-5490
Email: margulis@seas.ucla.edu

U.C. Water Resources Center
Technical Completion Report Project No. W-980

January 2006

Abstract

An ensemble-based radiometric data assimilation framework was developed to test the feasibility of snow water equivalent (SWE) estimation. Season-long synthetic experiments were run for conditions at Mammoth Mountain were passive microwave observations at SSM/I and AMSR-E frequencies and synthetic broadband albedo observations were assimilated simultaneously in order to update snowpack states in a land surface model using the Ensemble Kalman Filter (EnKF). The effects of vegetation and atmosphere are included in the radiative transfer model (RTM). The Land Surface Model (LSM) was given biased precipitation to represent typical errors introduced in modeling, yet was still able to recover the true value of SWE with a seasonally-integrated RMSE of only 2.95 cm, despite a snow depth of around 3 m and the presence of liquid water in the snowpack. This ensemble approach allows for investigating the complex theoretical relationships between the snowpack properties and the observations, and exploring the implications of these relationships for the inversion of remote sensing measurements for estimating snowpack properties. The contributions of each channel to recovering the true SWE were computed, and it was found that the low frequency 10.67 GHz AMSR-E channels contain information even for very deep snow. The effect of vegetation thickness on assimilation results was explored. Results from the assimilation were compared to those from a pure modeling approach and from a remote sensing inversion approach, and the effects of measurement error and ensemble size were investigated.

1. Introduction and Problem Statement

Many semi-arid regions of the globe, and specifically California, rely on snowmelt and the resulting runoff from the winter snowpack in local or regional mountains for the majority of their water supply. Additionally, because of the seasonal time lag between snow accumulation and subsequent snowmelt, an accurate characterization of the snowpack can provide significant lead-time predictions of water shortage or abundance for the upcoming year. As a result, the accurate characterization of accumulated winter snowpack and the resulting spring runoff is a critical task for water resource planners. This task is becoming even more important as economic and political pressures related to the allocation of scarce water supplies continue to increase (Daly et al., 2000).

For the purposes of planning, water resource engineers are ultimately interested in the integrated amount of water in the snowpack over a given watershed (snow water equivalent; SWE), which is a function of the depth and density of the snow. Both the depth and density of the snowpack can vary widely over space and time as a result of variations in precipitation, topography, incident radiation, etc. All of these factors contribute to a large variability in SWE over a basin (e.g. Cline et al., 1998a; Cline et al., 1998b; Liston, 1999). Despite the large variability in SWE, most operational efforts to determine snowpack water

supply still consist of snow surveys, where teams of people hike into the mountains, take snow cores at several specified points in a region, and manually determine the snow water equivalent at those points. The data are then compared to historical records of past surveys or used in empirical regression relationships to determine whether the water supply is below, at, or above average (Elder et al., 1991). Planning for the upcoming year is based almost entirely on these point-scale estimates and empirical relationships that rely on the consistency of snow cover from year to year. Furthermore, these snow surveys can be costly, dangerous to the surveyors, and are subject to yield inaccurate results when extrapolated to the entire basin.

The goal of this research project was to perform initial feasibility tests of an innovative approach to the estimation of basin-wide snow water equivalent by optimally combining remote sensing observations with physically-based hydrologic models using an advanced data assimilation technique.

2. Objectives

The goal of this particular study was prove the feasibility of the Ensemble Kalman Filtering (EnKF) data assimilation approach for snowpack characterization using multi-spectral remote sensing observations. The project is novel not only in its use of an advanced data assimilation scheme, but in the combination of remote sensing observations used. In this project, we not only incorporated the SSM/I microwave frequencies (19, 37 GHz dual polarization), which have been used in past snow remote sensing studies, but also lower frequency measurements (6.9 and 10.7 GHz dual polarization), which are available from the Advanced Microwave Scanning Radiometer (AMSR-E) instrument on NASA's recently launched AQUA satellite (AMSR-E also includes observations at 19, 24, 37 GHz). The lower frequency observations add additional information about the snowpack and are less attenuated by the atmosphere. In addition to the microwave measurements, visible, near-infrared, and thermal infrared observations and are included (during clear-sky conditions) from the Moderate Resolution Imaging Spectroradiometer (MODIS) instrument aboard NASA's Terra and Aqua satellites, which adds direct information about the snow surface albedo and temperature (Wan and Dozier, 1996; Wan and Li, 1997). This suite of instruments not only provides different spectral observations, but the observations are available at varying spatial and temporal resolutions. A major hypothesis of the work is that the synergistic benefits of using several remote sensing observations can significantly improve the estimation of snowpack characteristics.

The currently used methods for estimating snow properties from remote sensing observations can be classified as retrieval, or direct inversion, algorithms, where empirical or semi-empirical regression relationships between the remotely sensed measurement and parameter of interest are inverted. These techniques are fundamentally different from the data assimilation approach used in this study. These direct inversions can often fail because of the empirical expressions used and/or the non-unique relationship between the parameters and observations.

Instead of a direct inversion, a probabilistic Bayesian approach can be taken, where prior information (probability distribution) about the system state (e.g. snowpack characteristics) is updated using the information gained from an observation of the system. This is in fact the philosophy of data assimilation algorithms, which attempt to combine observations of the system with physical estimates provided by models (taking into account the uncertainty in both) in order to yield optimal estimates of the system states (McLaughlin, 1995). The snow studies to date that have come closest to this approach are Wilson et al. (1999) and Chen et al. (2001), who used a neural network inversion technique to obtain point-scale SWE estimates that are constrained with a physical model. The approach used here provides a significant step forward by implementing an advanced integrated data assimilation system that will ultimately be able to:

- use multiple remote sensing observation types (microwave and thermal infrared) in conjunction with a physical snow model to estimate SWE
- takes into account model and measurement errors
- provide estimates of the uncertainty (error bounds) of the SWE estimates, which are an essential piece of information for water resource planners
- provide downscaled estimates of SWE (i.e. at 1 km resolution) from coarse (i.e. 25 km resolution) remote sensing observations

The data assimilation methodology that was implemented is described fully below.

3. Procedure

In general, data assimilation algorithms try to characterize the true state of a system by systematically merging multiple sources of information (remote sensing and ground-based observations, physical process models, etc.). In this study the Ensemble Kalman Filter (EnKF) technique is used. The EnKF is a natural application of Bayesian estimation concepts (Jazwinski, 1970). Detailed discussions are provided in Evensen (1996), Houtekamer and Mitchell (1998, 2001), Reichle et al. (2002), and Margulis et al. (2002). The basic concepts may be illustrated if we consider a vector $y(t)$ composed of N_y uncertain hydrologic states. In our application, these states include snowpack characteristics within each pixel of a computational grid. The basic goal of the data assimilation procedure is to estimate these uncertain states from available radiobrightness and meteorological measurements.

A land surface snow model with uncertain inputs describes the evolution of the true states. This model is generally based on mass and energy conservation principles and can be written concisely as a vector-valued discrete-time state equation:

$$y(t) = A[y(\tau), \alpha, u(\tau), \omega(\tau), t, \tau] \quad t > \tau \geq 0 \;;\; y(0) = y_0(\alpha) \qquad (1)$$

where $y(t)$ is the N-dimensional state vector (e.g. discretized snowpack characteristics); α is a vector of time-invariant model parameters (e.g. soil or vegetation characteristics); $u(t)$ is a vector of time-dependent model forcing inputs (e.g. precipitation, air temperature, etc.); and $\omega(t)$ is a vector of time-dependent model errors. These equations describe how the state of the snowpack evolves in time over the basin from an initial condition $y(0)$ subject to specified forcing. Parameter and forcing errors can be accounted for probabilistically through the time-dependent model error term $\omega(t)$.

For this study, we used the Simple Snow-Atmosphere-Soil (SAST) transfer model which is an intermediate-complexity, 3-layer energy-balance snow scheme (Sun and Xue 1999). The SAST prognostic variables include enthalpy (related directly to snow temperature and density), snow water equivalent and snow depth. The model takes into account compaction due to destructive metamorphism, overburden and snow melting (Sun and Xue 1999). The default grain diameter and albedo parameterizations described in Sun and Xue (1999) are not detailed enough for this study. Due to the sensitivity of microwave emission and albedo to grain size (Armstrong, 1993; Nolin and Dozier 2000), a prognostic estimate of the grain size is required. Hence we incorporated the dynamic grain diameter model of Jordan (1991) into SAST. Additionally, the albedo parameterization was modified to include a dependence upon the grain diameter (Jordan, 1991), which is similar to the albedo estimate given in Marks and Dozier (1992). Based on the modified model, the state variables used in this study are snow depth and ground surface temperature in addition to snow density, temperature, grain size and volumetric water content in the three snowpack layers, for a total of fourteen state variables.

For this study we assume that the statistical properties of all random inputs are specified. In particular, the nominal (mean) values of precipitation and other time-dependent inputs (windspeed, air temperature, etc.) are interpolated from available ground-based micrometeorological measurements and the nominal values of soil and vegetation properties are derived from field observations. The covariances of these inputs are assigned reasonable values based on observed variability.

In order to estimate system states from microwave radiobrightness and thermal infrared measurements we need a radiative transfer model that describes how the observations are related to the snowpack and land surface characteristics. This model can be concisely expressed as a vector-valued discrete-time measurement equation:

$$z_i = M[y, \alpha, u, v_i, t_i] \quad ; \quad i = 1,...m \tag{2}$$

where z_i represents a vector of predicted measurements at time t_i, v_i is a vector of random measurement errors, and the nonlinear measurement operator M is a diagnostic equation which relates the model states to the observations. The measurement error may be additive, multiplicative, or of some other form, as required in a given application. In addition to the radiative transfer models, M may also account for differences in scale between the discretized states and

observations, any necessary atmospheric attenuation corrections, and the use of different observations at different times.

Three radiative transfer models (emission of the snowpack, and attenuation by the vegetation and atmosphere) must be employed in order to predict the satellite observation. The emission of microwave radiation from snowpacks has been investigated extensively. For this study, we have chosen the Microwave Emission Model of Layered Snowpacks (MEMLS; Wiesmann and Mätzler, 1999). MEMLS is a multi-layer model based on radiative transfer theory but accounts for multiple-scattering effects within the snowpack by using a spatial correlation function to model snow structure (Mätzler et al., 2000; Mätzler, 1997). The model description for computing scattering and absorption coefficients has been tested on many snow samples (Wiesmann et al., 1998) and validated against actual snow packs (Wiesmann and Mätzler, 1999). The vegetation is modeled according to Wegmuller et al. (1995), following the approach given in Tigerstedt and Pulliainen (1998). The reflectivity and transmissivity of individual leaves is based on the geometrical optics approach, taking into account the inhomogeneity of the electric field within the vegetation. The clear-sky atmosphere is modeled according to Ulaby et al. (1981) as implemented in Tigerstedt and Pulliainen (1998). Absorption by oxygen and water vapor are computed assuming a typical exponential relationship for water vapor and pressure profiles, and a simple expression for the temperature profile.

When we use data assimilation in a filtering/forecasting mode we seek the best estimate of $y(t)$, given the set of all measurements $Z_m = [z_1, z_2, \ldots, z_m]^T$ taken through time $t_m \leq t$. A filtering approach is ideally suited for the goal of estimating SWE for water resource planning, where we want an accurate characterization of the snowpack at the end of winter (just before the onset of spring snowmelt), conditioned on remote sensing observations taken over the entire winter season. Since $y(t)$ is a random variable, everything we know about it for a given Z_m is contained in the conditional probability density function $f[y(t)|Z_m]$. The EnKF uses a Monte Carlo approach to describe how this density evolves over time (between measurements) and how it changes when new measurements are included. It does this by following individual realizations (or replicates) drawn from a small population (or ensemble). This process is illustrated in Figure 1.

At time t_0, the state vector $y^j(t)$ associated with replicate j is started with an initial condition $y_0(\alpha^j)$ derived from a synthetically generated realization α^j of the time-invariant input vector α (here $j = 1,\ldots N_R$, where N_R is the number of replicates included in the ensemble). The state vector for each replicate is propagated forward in time to the first measurement time t_1, according to (1). Synthetically generated values (α^j and $u^j(t)$) of the random inputs α and $u(t)$ are inserted into (1) as required. At t_1 each replicate is updated (or conditioned) to reflect the effect of the measurement z_1. The updated states, which are written $y^j(t_1|Z_1)$ to indicate their dependence on all measurements collected through t_1, become the initial conditions for the next time period $(t_1, t_2]$. This process continues sequentially: first a propagation step over each interval

between measurement times (e.g. t_i and t_{i+1}) and then an update step at each measurement time (e.g. t_{i+1}).

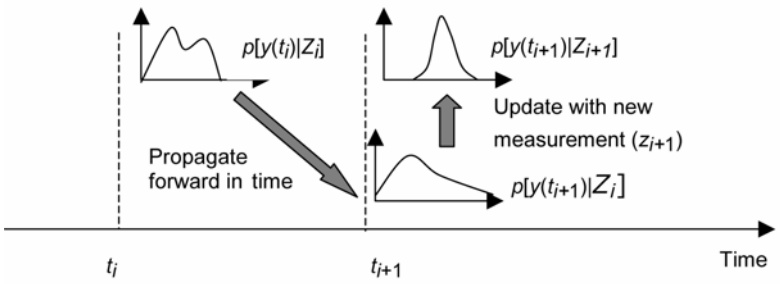

a) Evolution of the conditional probability density

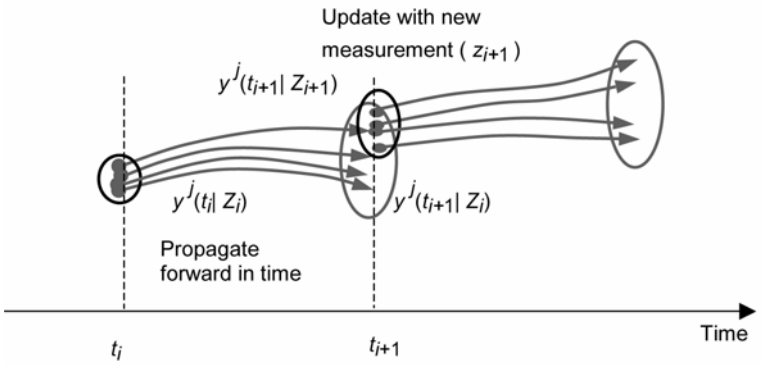

b) Evolution of random replicates in ensemble

Figure 1. Basic features of ensemble filtering: In a) the conditional probability density evolves between measurement times t_i and t_{i+1} and is updated with new information at time t_{i+1}. In b) individual realizations drawn from an ensemble characterized by this density evolve and are updated. The ensemble mean can be used as an estimate and the standard deviation as a measure of estimation accuracy.

Ideally, the update step of the sequential filtering procedure should be based on Bayes theorem, which specifies the probability density for the ensemble of updated replicates $y^j(t_{i+1}| Z_{i+1})$ at t_{i+1}. However, it is difficult to apply this theorem in practice, especially for large problems, unless the propagated state and the measurement vector are assumed to be jointly Gaussian. Then the propagated and updated densities are completely characterized by their means and covariances and Bayes theorem reduces to a pair of update equations for these two conditional moments. In the version of the ensemble Kalman filter used here each replicate is updated with the following expression (Margulis et al., 2002):

$$y^j(t_{i+1} \mid Z_{i+1}) = y^j(t_{i+1} \mid Z_i) + K\left\{ z_{i+1} + v_{i+1}^j - M[y^j(t_{i+1} \mid Z_i)] \right\} \qquad (3)$$

where K is a weighting (or Kalman gain) matrix derived from the measurement operator M and the sample covariance $C_{yy}(t_{i+1} \mid t_i)$ and $C_{yz}(t_{i+1} \mid t_i)$. It is the same for all replicates. The quantity $M[y^j(t+1) \mid Z_i]$ appearing in the update equation is the filter's prediction of the measurement obtained at t_{i+1}, given all information collected through t_i. The update depends on the difference between the actual and predicted measurements. A schematic of the merging of model inputs, predictions, and observations via the EnKF data assimilation approach is shown in Figure 2.

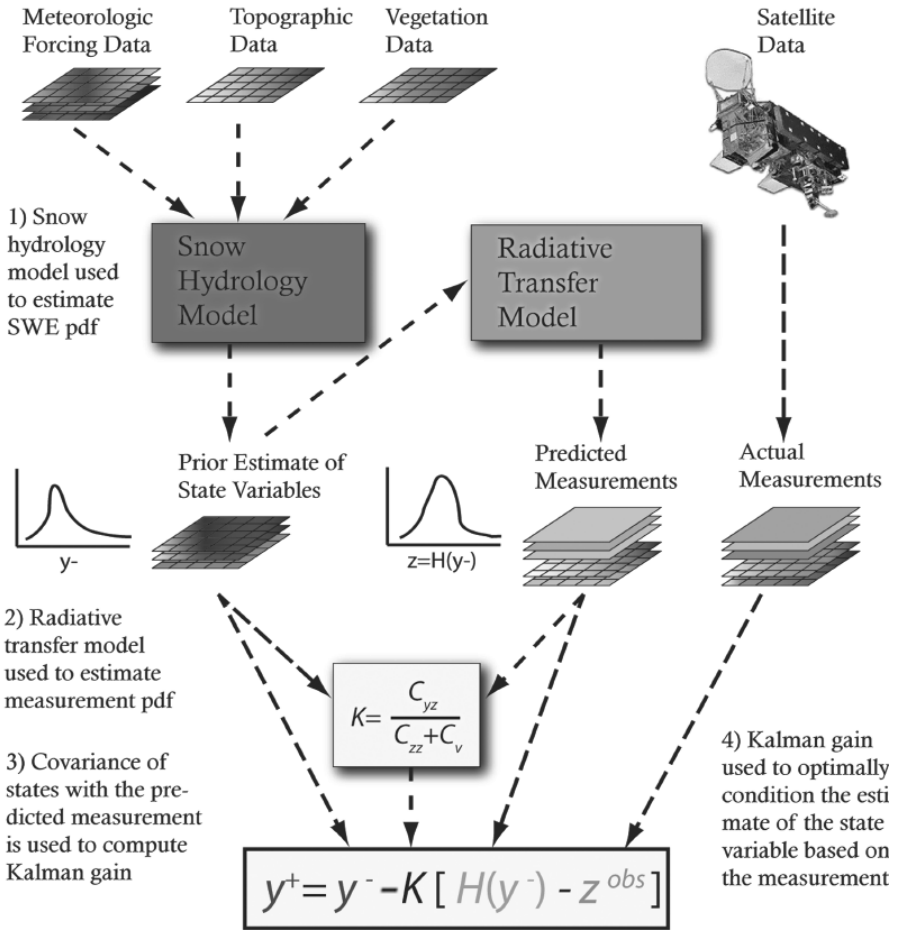

Figure 2. Schematic of EnKF methodology used for snowpack characterization. The snow model and radiative transfer model are used to generate prior distributions of predicted model states and measurements and to compute the Kalman gain *K*. The actual observations are used along with the Kalman gain to update the prior states.

When the Gaussian assumption used in the update procedure is correct, the EnKF algorithm outlined above gives an increasingly accurate characterization of

the conditional probability density $f[y(t)|\ Z_m]$ as the number of replicates is increased. From this density one could compute means, covariances, and other distributional quantities of interest. However, in land surface applications the Gaussian assumption is generally imperfect because the nonlinearities in the state and measurement equations tend to produce complex $y(t)$ distributions. Consequently, the EnKF only approximates $f[y(t)|Z_m]$. However, estimates based on this approximation are quite useful since the propagated ensemble members used to derive the sample covariance are affected by nonlinearities in the state equation.

The practical value of the EnKF approach has been show in recent soil moisture estimation studies (Reichle et al., 2002; Margulis et al., 2002). It should be noted that the EnKF approach makes fewer assumptions and is more flexible than most alternatives, including the extended Kalman filter (e.g. Galantowicz et al., 1999), which uses a linearized model during the propagation step, and variational methods (Reichle et al, 2001a, 2001b; Margulis and Entekhabi, 2003, 2004), which require the development of an adjoint of the particular forward model being used. Alternatively, the EnKF, with its modular approach, can be easily used with "off-the-shelf" models, making its use by the operational community much easier than other data assimilation techniques.

4. Results

4.1 Description of Experimental Setup

A necessary first step in a new application of data assimilation methodology is a synthetic experiment which allows for testing the feasibility of the approach in a controlled environment where the "true" state is known. In this study, we used the model in a lumped framework and focus on the complicated interactions between snow states and multi-frequency observations. A later study will apply the method for a spatially distributed case over a large basin.

The experimental setup is especially designed to evaluate whether errors in forcing data may be overcome by assimilating radiometric observations using the EnKF. To this end, point-scale forcing data was obtained from the Mammoth Mountain Energy Balance Station (MMEBS) for the 1993-94 winter (Davis et al., 1984) in order to drive the snow model. We must make some assumptions regarding the error statistics of these nominal forcing data. Due to the common occurrence of undercatch in snow precipitation data sets and especially in mountainous terrain, we included a positive bias when computing the precipitation for the true simulation: It was specified that, on average, the measured value was 50 % of the actual precipitation. This mimics the situation in which the measured value is biased by gage undercatch.

To provide a benchmark for evaluating the filter estimate, we ran the model in "open loop" mode, i.e., without the benefit of the observations. The "open loop" simulation is given the nominal forcing data and parameter values, so that it receives, on average, only 50 % of the true simulation precipitation. The

EnKF replicates also receive an average of 50 % of the true precipitation as well as randomly perturbed grain growth parameter values. In this test, the collection of observations used in the assimilation are brightness temperatures at several passive microwave frequencies (available from SSM/I and/or AMSR-E) as well as broadband albedo (available from MODIS), all computed synthetically at a single point from snow states generated by SAST. The observations are corrupted assuming that the standard deviation of the passive microwave measurement error and the broadband albedo measurement error can be characterized as white Gaussian noise with a standard deviation of 2 K and 5 %, respectively. We chose an ensemble size of 100 replicates to represent the pdf of the state and measurement variables.

The AMSR-E instrument on the Aqua platform has equatorial cross-over times around 1 AM and 1 PM daily. For simplicity, it is assumed that all microwave observations are available at 1 AM and the albedo observations at the 1 PM overpass. There are seven SSM/I channels including 19.35 GHz, 22.235 GHz, 37.0 GHz and 85.5 GHz at vertical and horizontal polarizations, except the 22.235 GHz channel which has only the vertical polarization. AMSR-E has twelve channels, including 6.925 GHz, 10.65 GHz, 18.7 GHz, 23.8 GHz, 36.5 GHz and 89 GHz, all at both horizontal and vertical polarizations. All fourteen snow states are updated at each measurement time, and the snow water equivalent may then be computed from the snow depth and snow density.

Implementing the methodology described above, the EnKF was run under a variety of conditions for this lumped model test using forcing data from the MMEBS for the 1993-94 winter. Results below are grouped by the subset of frequencies assimilated; results from assimilation of observations at SSM/I frequencies are discussed first, followed by results from assimilation of AMSR-E frequencies and results from simultaneous assimilation of AMSR-E frequencies and broadband albedo. For each frequency subset, we review the basic filter results of the EnKF estimate of the SWE, which is of primary interest. All of these initial tests are for the bare snow case. The impact of vegetation on these results is discussed below. Sensitivity tests examining the effects of the measurement error and the ensemble size on the EnKF estimate are presented at the end of this section.

4.2 Performance of EnKF Using SSM/I Frequencies

The snow depth and snow density (for the bottom snow layer) estimated from the assimilation of synthetic passive microwave observations at SSM/I frequencies are shown in Figure 3. The true snow depth grows rapidly in the first two weeks of December, and is approximately 1meter until February. Snow events during February increase the depth to over 3 meters, after which the snow compacts (due to destructive metamorphism) to approximately 2 meters. The sharp drops in the bottom layer snow density are due to precipitation events. (Throughout the text, the bottom layer is denoted by a '1' subscript and the surface layer by a '3' subscript). As expected, the result of the precipitation bias leads to underestimation of snow depth in the open loop case. It is immediately clear that the EnKF estimate greatly improves upon the biased open-loop model run for

both snow depth and density. These states are used together with the upper layer densities (not shown) to compute the SWE, discussed below.

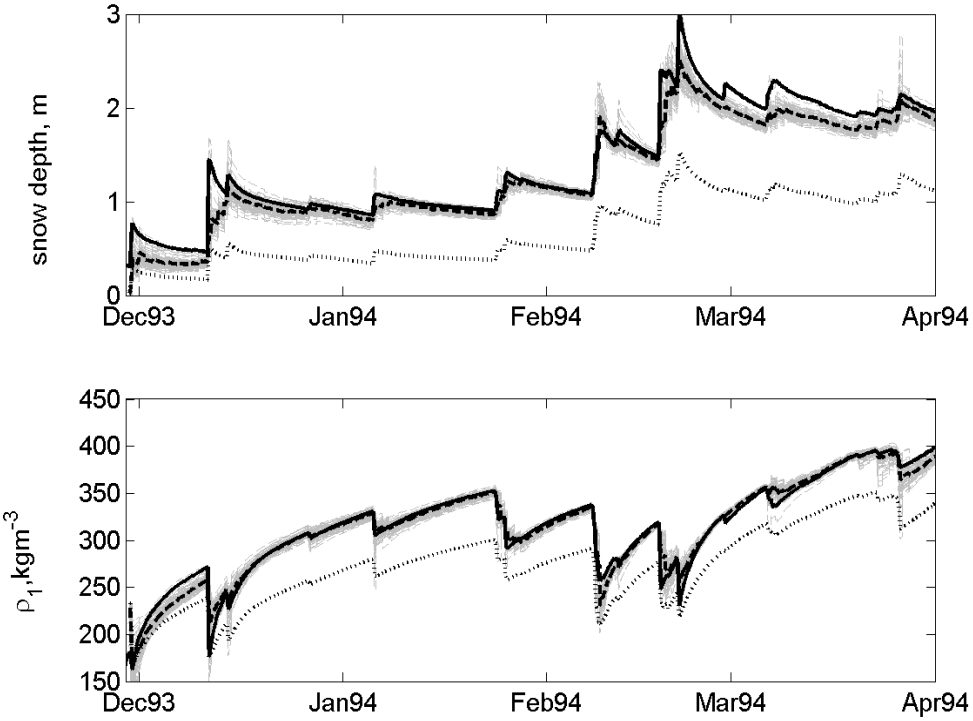

Figure 3. Snow depth and bottom layer density predicted by EnKF methodology. The truth is the solid line, the open-loop is the dotted line, the faint dotted lines are individual replicates and the EnKF estimate (ensemble mean) is the dashed line. Snow density in the upper two snow layers is also estimated by the EnKF, but these estimates are not shown since both the SWE and the predicted observations depend mostly on the bottom layer density.

Two additional state variables, grain diameter (Figure 4) and the volumetric liquid water content (melted fraction) of the snowpack (Figure 5) are shown. Accurate estimates of these variables are required in order to accurately predict the observations using the RTM. From Figure 4, it is clear that the grain diameter estimates are qualitatively much closer to the truth than the open-loop values throughout the winter. For much of the snow season, there is no liquid water present in the snowpack, and the bottom layer (not shown) is dry throughout the snow season. Liquid water for two weeks late in the snow season for the two surface layers are shown in Figure 5. An important advantage of the EnKF over retrieval methods, is that the SWE estimate does not degrade significantly when liquid water is present in the snowpack, since some ensemble members should have some liquid water present, and this will be reflected in the ensemble of predicted observations. Furthermore, if a measurement contains little or no SWE information, the update is, by definition, small so that the posterior estimate is equal to the prior estimate.

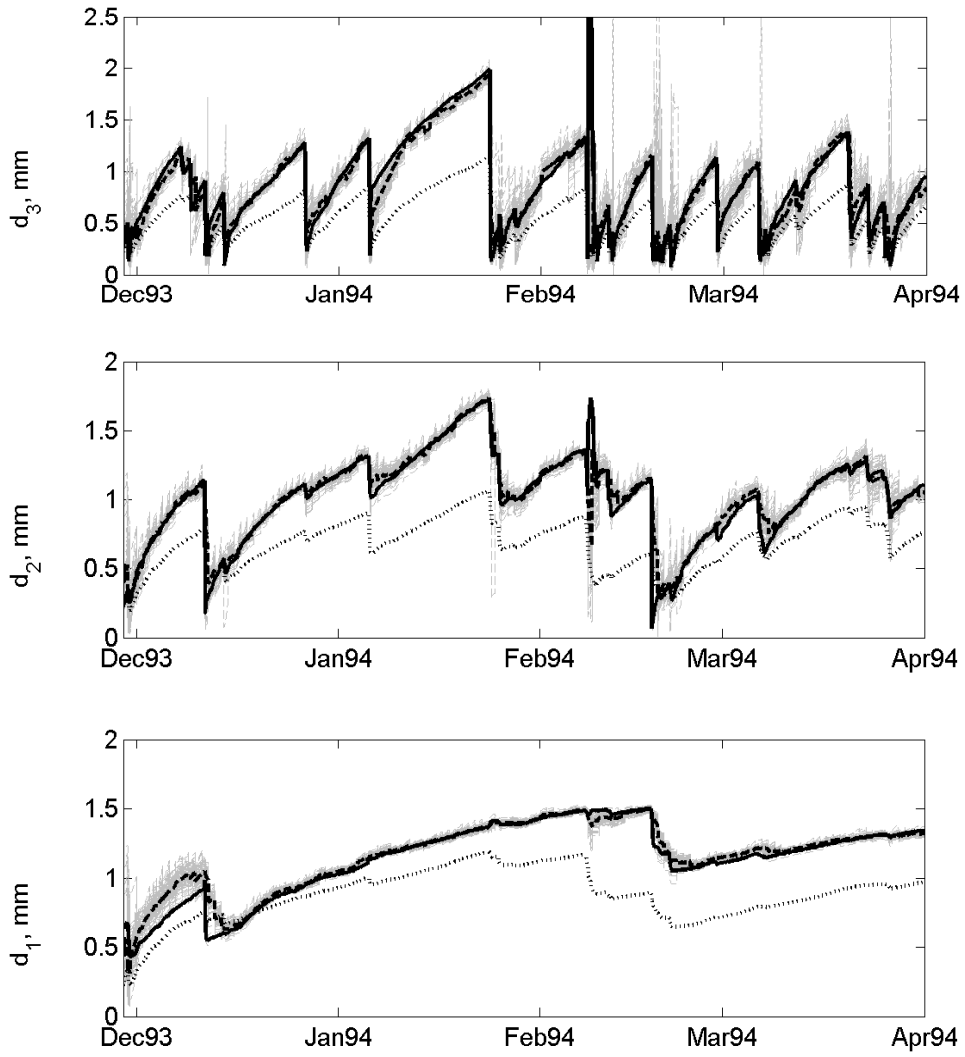

Figure 4. Grain diameter for each layer estimated by EnKF methodology. The truth is the solid line, the open-loop is the dotted line, the faint dotted lines are individual replicates and the EnKF estimate (ensemble mean) is the dashed line.

From the depth and density state variables, the SWE is computed and shown in Figure 6. The estimate follows the truth closely through mid-February, after which there is a low bias. This persistent low bias is due in part to the fact that the measurements begin to saturate for deep snow. From Table 1, the ensemble mean estimate has a season-averaged bias of 3.4 cm, and RMSE of 4.0 cm, which is an 85 % reduction of the the open-loop RMSE of 27.1 cm.

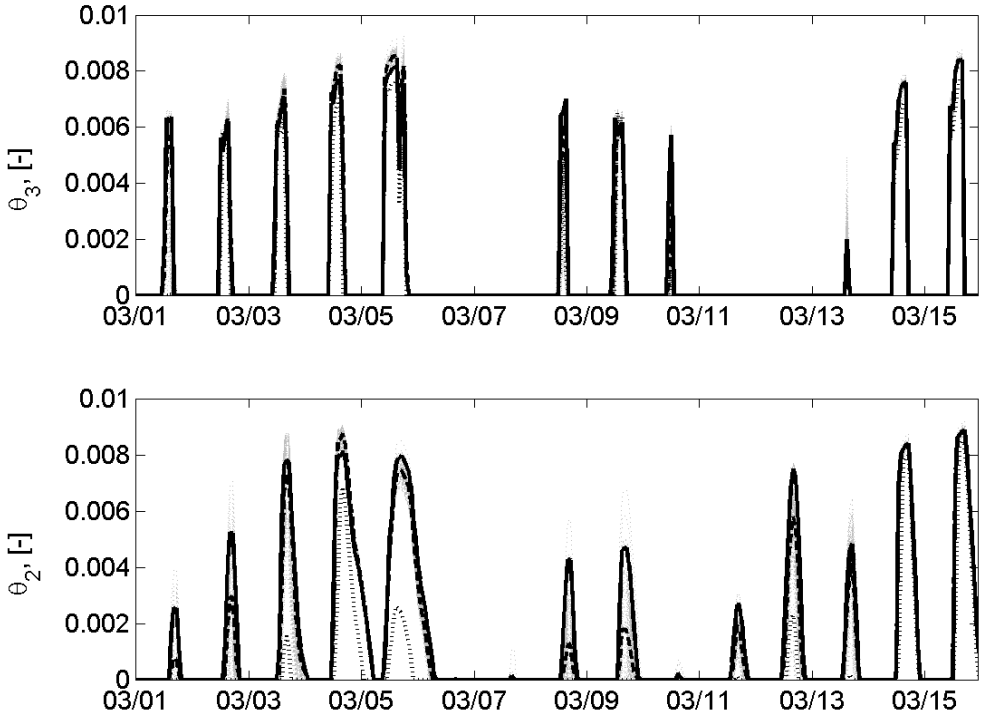

Figure 5. Dimensionless liquid water content of the snowpack for the upper layers estimated by EnKF methodology for two weeks in March. The truth is the solid line, the open-loop is the dotted line, the faint dotted lines are individual replicates and the EnKF estimate (ensemble mean) is the dashed line. No liquid water was present in the bottom layer (θ_1=0).

Table 1. The Bias and RMSE of the SWE estimate for assimilating different synthetic observations and for the open loop simulation.

	Bias	**RMSE**
Open Loop	25 cm	27.1 cm
SSM/I	3.4 cm	4.0 cm
AMSR-E	2.0 cm	3.2 cm
AMSR-E and MODIS	1.2 cm	2.6 cm

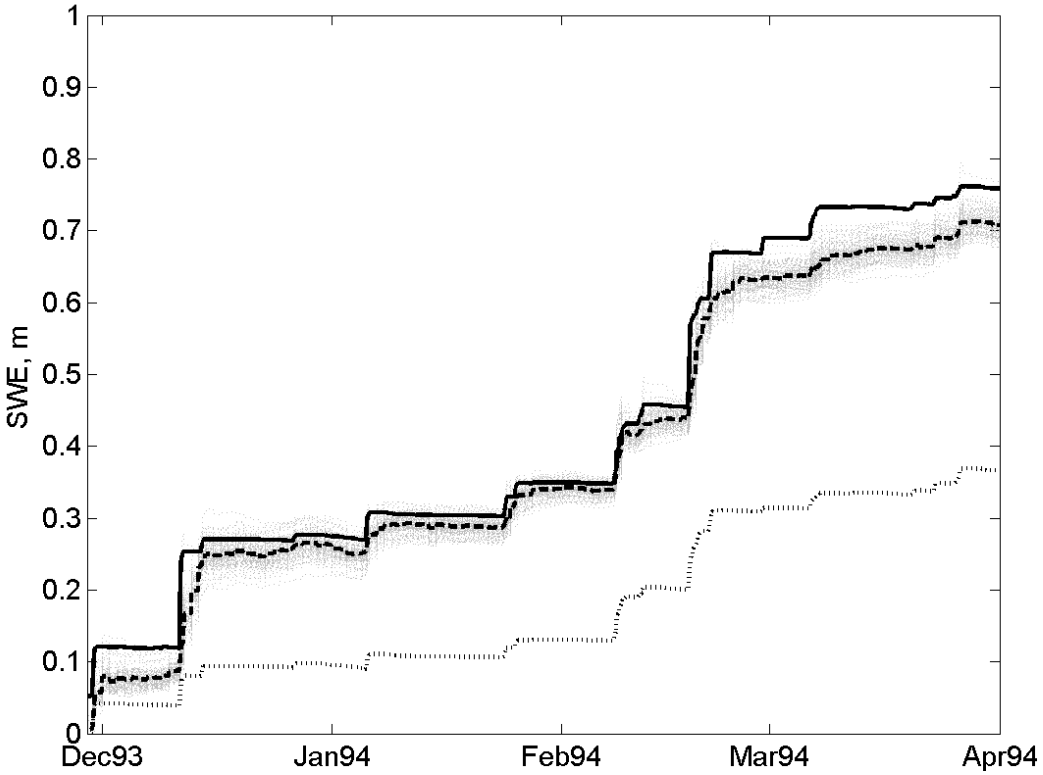

Figure 6. Snow water equivalent estimate obtained by assimilating synthetic observations corresponding to SSM/I frequencies. The truth is the solid line, the open-loop is the dotted line, and the EnKF estimate is the dashed line.

In addition to comparing the EnKF performance to the open-loop case, it is instructive to use the synthetic measurements at the SSM/I channels to compare results to a well-known retrieval algorithm for estimating snow depth. Figure 7 shows the SWE computed by the EnKF and the Chang (1987) algorithm. Since the retrieval methodology was only designed to work for snow with a depth less than one meter, we compared the results for the months of December and January only. Though not applicable during February and March, the retrieval algorithm provides a good benchmark for the effectiveness of the EnKF estimate. The RMSE for the Chang algorithm is 13.8 cm, compared to an RMSE of 3.2 cm for the EnKF estimate during December and January. Furthermore, the retrieval algorithm does not capture the temporal changes in the snowpack over this period, highlighting an important advantage of the EnKF over retrieval algorithms in general.

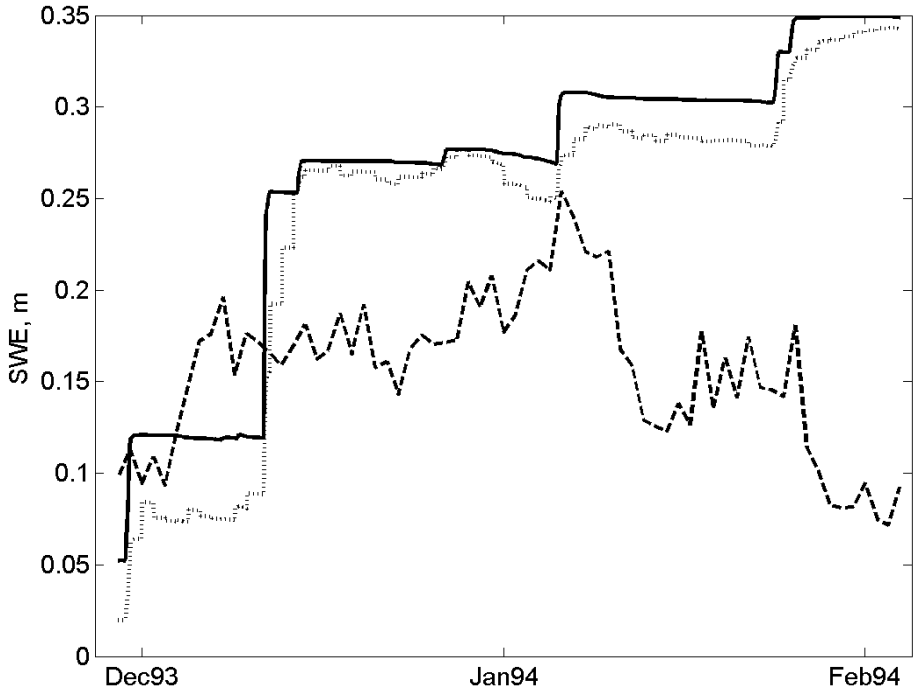

Figure 7. True SWE and results from the EnKF and a common microwave inversion algorithm. The truth is the solid line, the Chang (1987) algorithm is the dotted line, and the EnKF estimate is the dashed line.

4.3 Performance of EnKF Using the AMSR-E frequencies

One of the hypotheses of this study is that the additional low frequency observations from the AMSR-E sensor could provide additional information about the snowpack characteristics at greater depths. From Figure 8, the EnKF SWE estimate using the AMSR-E frequencies has improved somewhat over the SSM/I case. The estimate is excellent throughout December, January and February. Near the end of February, however, we see the same low bias in the snow water equivalent that we observed previously. Nevertheless, the addition of the low frequency 6.925 GHz and 10.65 GHz channels apparently improve the estimate inasmuch as the RMSE from Table 1 for the estimate is only 3.2 m, which is 0.7 cm or 19 % less than the RMSE for the estimate using the SSM/I frequencies.

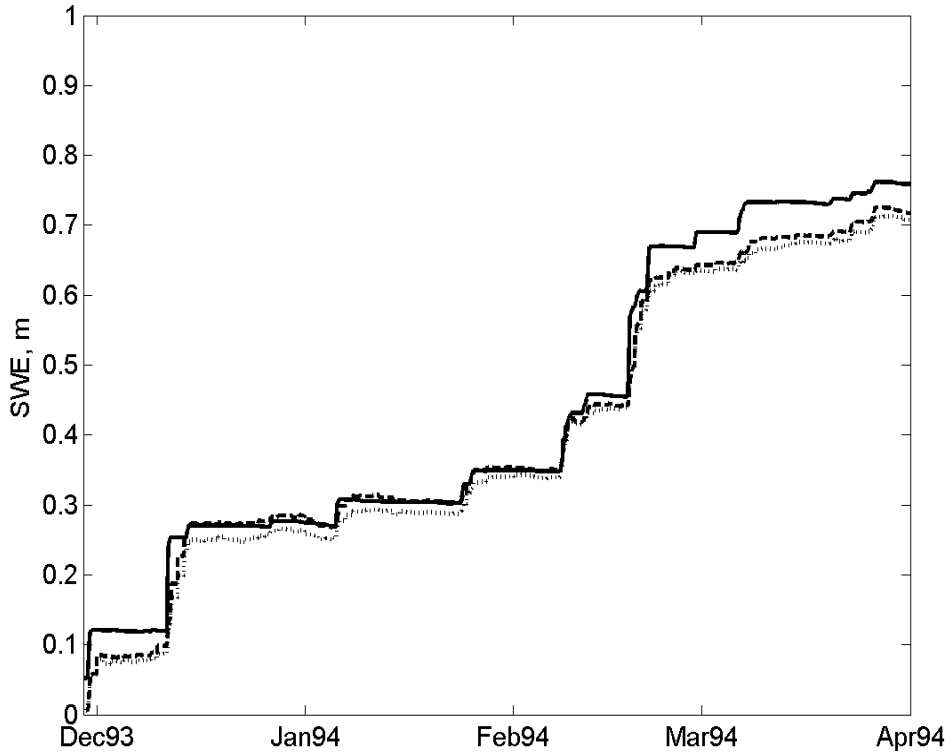

Figure 8. Snow water equivalent estimates obtained by assimilating different subsets of passive microwave frequencies are shown. The truth is the solid line, the result using SSM/I is the dotted line and the result using AMSR-E is the dash-dot line. The vertical lines show the update times on December 13, February 9 and March 9, which are discussed in detail.

4.4 Impact of addition of MODIS broadband albedo

We next considered assimilation of synthetic passive microwave observations at AMSR-E frequencies and broadband albedo observations simultaneously. From Table 1 the Bias is reduced from the AMSR-E case by 41 % or 0.8 cm and the RMSE is only lower 0.6 cm or 18 % less than the estimate made without the albedo observations. These results support the idea that there is a synergistic benefit between assimilation of both passive microwave and visible / NIR observations. Furthermore, the spatial resolution of the MODIS observations have a nominal value of 500 m, while the AMSR-E observations have resolutions ranging between 5 and 60 km. We hypothesize that the MODIS albedos will contribute to accurate grain diameter and SWE estimates at relatively high spatial resolution in the spatially distributed case. This hypothesis will be tested in follow-on work.

4.5 Effects of Vegetation

It is well known that vegetation severely attenuates passive microwave signals (e.g., Foster et al., 2005). For this reason, we repeated the assimilation of

AMSR-E frequencies with different thicknesses of vegetation, with wet biomass values ranging from 1.0 kg m^{-2} to 3.0 kg m^{-2}. The results can be seen in Figure 9; it is clear that with thicker vegetation, measurements contain less information about SWE, and the filter results begin to converge to the open-loop results. The Bias and RMSE of the SWE for each of these simulations is shown in Table 2; even for a wet biomass of 1.0 kg m^{-2}, the RMSE has already more than doubled over the no vegetation case. However, even for thick vegetation with a wet biomass of 3.0 kg m^{-2} the RMSE value of 18.51 cm is still 26 % less than the open-loop RMSE of 25 cm.

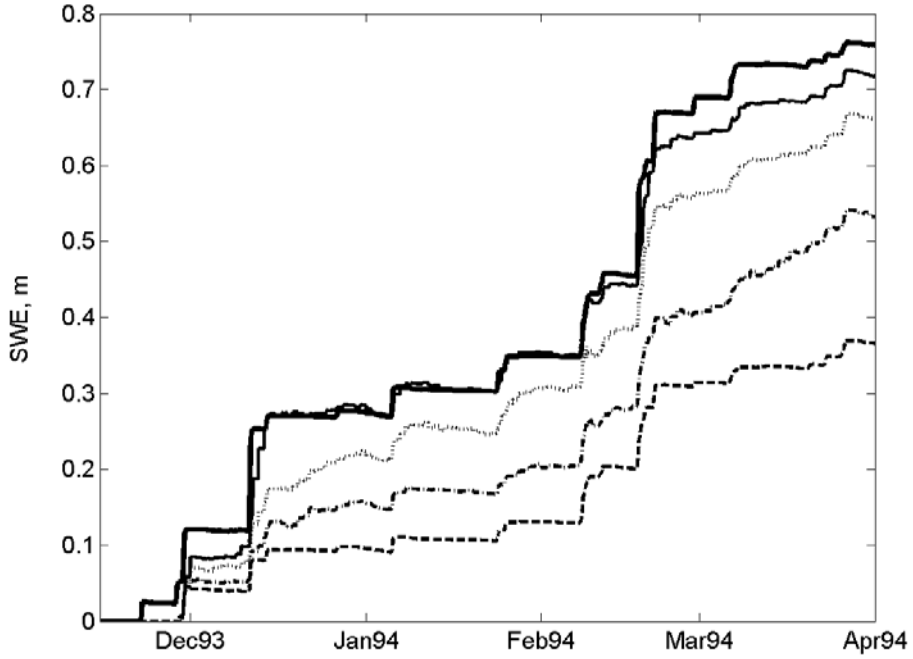

Figure 9. The effects of vegetation thickness are shown. The true simulation is the heavy solid line, the thin solid line is the assimilation results without vegetation, the dotted line is for wet biomass of 1.0 kg m^{-2}, the dash-dot line is for 3.0 kg m^{-2}, and the dashed line is the open-loop simulation.

Table 2. The Bias and RMSE of SWE estimates are shown for various vegetation thickness.

Wet Biomass, kg m^{-2}	Bias	RMSE
0	2.0 cm	3.2 cm
0.9	8.0 cm	8.6 cm
1.9	12.4 cm	13.2 cm
2.9	17.3 cm	18.5 cm

4.5 Sensitivity Study

In order to evaluate the effect of the measurement error on the performance of the filter, we performed parallel runs assimilating synthetic AMSR-E measurements only using measurement errors of 1 K, 2 K and 4 K in brightness temperature. From Table 3, even with the higher 4 K error, the RMSE is still significantly better than both the open loop RMSE (27.1 cm) and the early winter retrieval RMSE (10 cm) cited above. The RMSE in the case of 4 K standard error is 6.36 cm, which is 3.2 cm or twice as large as the RMSE with 2 K error. The bias is nearly three times as large if the error is 4 K, so the results are quite sensitive to measurement error).

Table 3. The RMSE and Bias of the SWE estimate for different assumed values of the standard deviation of the measurement error.

Standard Meas. Error	Bias	RMSE
1 K	0.8 cm	2.2 cm
2 K	2.0 cm	3.2 cm
4 K	5.7 cm	6.4 cm

We also examined the effect of ensemble size on the filter performance. The estimate of SWE based on assimilation of AMSR-E frequencies was computed for various numbers of replicates, and the results are shown in Table 4. It is clear that ensemble sizes of less than 25 lead to higher error, as the RMSE of the 5 replicate run is 7.0 cm. The RMSE of the 50 and 100 replicate runs are 2.9 cm and 3.2 cm, respectively, so that we can see there is a threshold, between 25 and 50 replicates, above which there are diminishing returns.

Table 4. The Bias and RMSE of the SWE estimate based on assimilation of AMSR-E frequencies are shown for different numbers of replicates, n_r.

n_r	Bias	RMSE
5	6.3 cm	7.0 cm
25	3.1 cm	3.7 cm
50	1.1 cm	2.9 cm
100	2.0 cm	3.2 cm

5. Conclusions

A new method for estimating SWE using synthetic multi-frequency remote sensing observations was tested. The EnKF radiometric data assimilation scheme was used to recover the true snowpack states (most notably SWE). It is applicable to deep snow with liquid water present. The EnKF run was performed using artificially biased meteorological forcing data, such that the average ensemble replicate received only half the precipitation that the true state received. The results are very encouraging, in that the synthetic microwave observations using all twelve AMSR-E channels contained sufficient information to recover the true SWE to within an RMSE of approximately 3 cm compared to the maximum SWE of 80 cm and maximum snow depths of greater than 3 m. A method for evaluating the contribution of each channel during an update was developed, and the integrated contribution of each channel was determined. It was confirmed that in the context of this data assimilation experiment, at least some passive microwave channels (for example the 10.65 GHz channel) still contain valuable information even in the case of deep snow. The 18.7 GHz and 23.8 GHz channels add much less information than the 10.65 GHz channel in this experiment. Assimilating albedo observations in addition to passive microwave measurements improved the RMSE by nearly twenty percent; furthermore, it is anticipated that these albedo observations will play a significant role in refining the surface grain diameter estimate in the spatially distributed case. A thin layer of vegetation more than doubles the SWE RMSE; but even when subject to thick vegetation, the filter estimate is much improved over the open loop case.

The effects of measurement error and ensemble size on the EnKF efficiency in terms of the RMSE of the SWE, were also evaluated. The filter performance is quite sensitive to assumed measurement error, and there is a minimum number of replicates (approximately 50) that are needed in order to achieve accurate results and above which there are diminishing returns on the added computational expense of the ensemble propagation. The next logical step in this research is to apply this methodology to a spatially distributed test case. For the distributed case, the various resolutions of the different microwave frequencies and the MODIS albedo will all come into play, leading to additional potential synergism between observations. Another possible extension of this work would be to assimilate active remote sensing observations, which generally have higher spatial resolution and are beginning to be utilized in inversion schemes for estimating SWE (Marshall et al., 2004). Ultimately, we anticipate the assimilation of real AMSR-E, SSM/I and MODIS observations. The ensemble methodology could eventually be applied to the very relevant problem of estimating snow mass in remote regions of the world where the need to drive hydrologic models using meteorological forcing data derived from remote sensing instruments requires careful accounting of additional input uncertainties.

Acknowledgments

We would like to thank Yongkang Xue, Christian Mätzler, Jouni Pulliainen and Rachel Jordan for giving us their codes as well as their advice and support throughout this project. Logistical support and/or data were provided by the NASA investigation "Hydrology, Hydrochemical Modeling, and Remote Sensing in Seasonally Snow-covered Alpine Drainage Basins", the Donald Bren School of Environmental Science and Management at the University of California, Santa Barbara, the US Army Corps of Engineers Cold Regions Research and Engineering Lab (CRREL), and the Mammoth Mountain Ski Area.

6. References

Armstrong, R., A. Chang, A. Rango, and E. Josberger, 1993: Snow depths and grain size relationships with relevance for passive microwave studies, *Annals of Glaciology*, 17, 171-176.

Chang, A., J. Foster, and D. Hall, 1987: Nimbus-7 SMMR derived global snow cover parameters. *Annals of Glaciology*, 9, 39-44.

Chen, C.-T., B. Jijssen, J. Guo, L. Tsang, A.W. Wood, J.-N. Hwang, and D.P. Lettenmaier, 2001: Passive microwave remote sensing of snow constrained by hydrological simulations, *IEEE Trans. Geosci. Remote Sens.*, 39(8), 1744-1756.

Cline, D.W., R.C. Bales, and J. Dozier, 1998a: Estimating the spatial distribution of snow in mountain basins using remote sensing and energy balance modeling, *Water Resour. Res.,* 34(5), 1275-1285.

Cline, D., K. Elder, and R.C. Bales, 1998b: Scale effects in a distributed snow water equivalence and snowmelt model for mountain basins, *Hydrol. Process.,* 12, 1527-1536.

Daly, S.F., R. Davis, E. Ochs, and T. Pangburn, 2000: An approach to spatially distributed snow modelling of the Sacramento and San Joaquin basins, California*, Hydrol. Process.*, 14, 3257-3271.

Durand, M., and S. Margulis, 2006: Feasibility test of multi-frequency radiometric data assimilation to estimate snow water equivalent, *Journal of Hydrometeorology*. in press.

Elder, K., J. Dozier, and J. Michaelson, 1991: Snow accumulation and distribution in an alpine watershed, *Water Resour. Res.,* 27, 1541-1552.

Evenson, G., and P.J. van Leeuwen, 1996: Assimilation of Geosat altimeter data for the Agulhas Current using the Ensemble Kalman filter with a quasigeostrophic model, *Mon. Wea. Rev*., 124, 85-96.

Galantowicz, J. F., D. Entekhabi and E. G. Njoku, 1999:Tests of sequential data assimilation for retrieving profile soil moisture and temperature from observed L band radiobrightness, *IEEE Transactions on Geoscience and Remote Sensing*, 37(4), 1860-1870.

Houtekamer, P.L. and H.L. Mitchell, 1998: Data assimilation using an Ensemble Kalman filter technique, *Mon. Wea. Rev*., 126, 796-811.

Houtekamer, P.L. and H.L. Mitchell, 2001: A sequential ensemble Kalman filter for atmospheric data assimilation, *Mon. Wea. Rev*., 129, 123-137.

Jazwinski, A. H., 1970: *Stochastic Processes and Filtering Theory*. Academic Press.

Jordan, R., 1991: A one-dimensional temperature model for a snow cover: Technical documentation for SNTHERM. 89, U.S. Army Corps of Engineers, Special Report, 91-16.

Liston, G.E., 1999: Interrelationships among snow distribution, snowmelt, and snow cover depletion: Implications for atmospheric, hydrologic, and ecologic modeling, *J. Appl. Meteor.,* 38, 1474-1486.

Margulis, S. A., D. B. McLaughlin, D. Entekhabi, and S. Dunne, 2002: Land data assimilation and estimation of soil moisture using measurements from the Southern Great Plains 1997 field experiment, *Water Resources Research*, in press.

Margulis, S.A. and D. Entekhabi, 2003: Variational Assimilation of Radiometric Surface Temperature and Reference-Level Micrometeorology into a Model of the Atmospheric Boundary Layer and Land Surface, *Monthly Weather Review*, 131(7), 1272-1288.

Margulis, S.A. and D. Entekhabi, 2004: Boundary layer entrainment estimation through assimilation of radiosonde and micrometeorology data into a mixed-layer model, *Boundary-Layer Meteorology*, 110, 405-433.

Marks, D. and J. Dozier, 1992: Climate and energy exchange at the snow surface in the alpine region of the Sierra Nevada 2. Snow cover energy balance, *Water Resources Research*, 28(11), 3043-3054.

Marshall, H., Koh, G., and Forster, R., 2004: Ground-based frequency-modulated continuous wave radar measurements in wet and dry snowpacks, Colorado, USA: an analysis and summary of the 2002–03 NASA CLPX data, *Hydrological Processes*, 18, 3609-3622.

Mätzler, C., 1997: Autocorrelation functions of granular media with free arrangment of spheres, spherical shells or ellipsoids, *Journal of Applied Physics*, 81(3), 1509-1517.

Mätzler, C., A. Wiesmann, J. Pulliainen, and M. Hallikainen, 2000: Development of Microwave Emission Models of Snowpacks, *IEEE Geoscience and Remote Sensing Newsletter*, 115, 18-25.

McLaughlin, D., 1995: Recent developments in hydrologic data assimilation, *Rev. Geophys*. (supplement), 977-984.

Nolin, A. and Dozier, J. 2000: A Hyperspectral Method for Remotely Sensing the Grain Size of Snow, *Remote Sensing of Environment*, 74, 207-216.

Reichle, R., D. Entekhabi, and D. McLaughlin, 2001a: Downscaling of radiobrightness measurements for soil moisture estimation: A four-dimensional variational data assimilation approach, *Water Resour. Res.*, 37(9), 2353-2364.

Reichle, R., D. B. McLaughlin, and D. Entekhabi, 2001b: Variational data assimilation of microwave radiobrightness observations for land surface hydrologic applications, *IEEE Transactions on Geosci. and Remote Sens.*, 39(8), 1708-1718.

Reichle, R., D. McLaughlin, and D. Entekhabi, 2002: Data assimilation using an ensemble Kalman Filter technique, *Mon. Wea. Rev.*, 129, 123-137.

Sun, S., J. Jin, and Y. Xue, 1999: A simple snow-atmosphere-soil transfer model, *Journal of Geophysical Research - Atmospheres*, 104(D16), 19,587-19,597.

Tigerstedt, K., and J. Pulliainen, 1998: Retrieval of Geophysical Parameters with Integrated Modelling of Land Surfaces and Atmosphere, ESTEC Contract, No. 11706/95/NL/NB(SC).

Tsang, L., 1987: Passive remote sensing of dense nontenuous media, J. Electromag. Waves Appl., 1(2), 159-173.

Ulaby, F., R. Moore, and A. Fung, 1981: Microwave remote sensing, active and passive. Vol I. Addison-Wesley, Reading, MA.

Wan, Z. and J. Dozier, 1996: A generalized split-window algorithm for retrieving land-surface temperature from space, *IEEE Trans. Geosci. Remote Sens*., 34, 892-905.

Wan, Z., and Z.-L. Li, 1997: A physics-based algorithm for retrieving land-surface emissivity and temperature from EOS/MODIS data, *IEEE Trans. Geosci. Remote Sens*., 35, 980-996.

Wegmuller, U., C. Mätzler, and E. Njoku, 1995: Canopy opacity models, In Passive Microwave Remote Sensing of Land-Atmosphere Interactions: ESA/NASA International Workshop, Choudhury, B., Y. Kerr, E. Njoku, and P. Pampaloni, editors, p.375-387.

Wiesmann, A., and C. Mätzler, 1998: Radiometric and structural measurements of snow samples, *Radio Science*, 33(2), 273-289.

Wiesmann, A., and C. Mätzler, 1999: Microwave emission model of layered snowpacks, *Remote Sensing of Environment*, 70, 307-316.

Wilson, L., L. Tsang, J.-N. Hwang, C.-T. Chen, Mapping snow water equivalent by combining a spatially distributed snow hydrology model with passive microwave remote-sensing data, *IEEE Trans. Geosci. Remote Sens*., 37(2), 690-704.

7. List of Publications Resulting From Project

Durand, M. and S.A. Margulis, 2006: Feasibility test of multi-frequency radiometric data assimilation to estimate snow water equivalent, *Journal of Hydrometeorology*, in press.

Durand, M. and S.A. Margulis, 2005: Large-scale SWE Estimation: Optimal Use of Remote Sensing and Snow Modeling, Southwest Hydrology, 4(2), 20-21, 32.